Pramana – J. Phys. (2016) 87: 91
DOI 10.1007/s12043-016-1301-z

Pulse generation and compression using an asymmetrical porous silicon-based Mach–Zehnder interferometer configuration

SHU-WEN GUO and JIAN-WEI WU*

College of Physics and Electronic Engineering, Chongqing Normal University, Chongqing 401331, People's Republic of China
*Corresponding author. E-mail: jwwucn@gmail.com

MS received 19 November 2015; revised 4 February 2016; accepted 7 March 2016; published online 3 November 2016

Abstract. We propose an asymmetrical Mach–Zehnder interferometer (MZI) for efficient pulse generation and compression using porous silicon (PS) waveguide, fibre delay line and couplers. We show a pulse compression of about 0.4 ns at the output port with third-order super-Gaussian input pulse in ∼2 ns time duration and ∼40.3 W peak power level. Also, we show the possibility of obtaining compressed single- or double-pulse with judicious choice of various parameters like input peak power, delay time and input pulse width.

Keywords. Silicon nanophotonics; porous silicon waveguide; pulse generation and compression.

PACS Nos 42.70.Nq; 42.65.Wi; 42.65.Re

1. Introduction

Recently, silicon waveguides (SW) have attracted considerable attention owing to their potential applications in integrated optoelectronics. Using SWs, many optical functions, such as laser modulation [1], amplification [2], wavelength conversion [3], signal generation [4], soliton switching [5], and slow light [6], have been presented and demonstrated. All these functions are possible through the judicious exploitation of linear and nonlinear effects such as two-photon absorption (TPA), free carrier absorption (FCA), free carrier dispersion (FCD), self-phase modulation (SPM), cross-phase modulation (XPM), and Raman scattering (RS) exhibited by crystalline silicon. Silicon-on-insulator (SOI) technique is often adopted in various silicon-based elements. In SOI, a silica cladding surrounds the silicon waveguide having a core with high refractive index generally on the order of 3.5. As a result, the transmitted light can be tightly confined into a small chip region with micrometre dimension and higher optical intensity can be easily obtained even for low input optical power. On the other hand, this results in strong nonlinear process in crystalline silicon. It has been observed that porous silicon (PS) exhibits significant free carrier related nonlinear effects compared to the conventional crystalline silicon. PS has much short free carrier recovery time and enhanced FCA and FCD [7]. In addition, both TPA and Kerr coefficients in PS are slightly lower than those in crystalline silicon. Utilizing these prominent properties in this work, we propose a PS-based pulse generation and compression method as PS is one of the essential components in optical telecommunication systems.

2. Device and operation principle

The schematic diagram is illustrated in figure 1, where the device consists of two Y fibre couplers, a PS waveguide, and a fibre delay line. A third-order super-Gaussian pulse is introduced into the two arms of the MZI through a 50:50 Y coupler. Half of the initial energy is launched into the PS waveguide and the other half passes through the optical delay line. In the PS waveguide, amplitude and phase of the signal is nonlinearly modulated by nonlinear processes including TPA, FCA, FCD, and SPM. Due to weak nonlinearity, in the short fibre delay line, the amplitude and phase of the pulse do not change. Thus, significant phase difference occurs between the two output beams from the PS and the delay line. These beams are recombined again by a Y 50:50 coupler. Owing to their strong phase difference, effective interference behaviour can

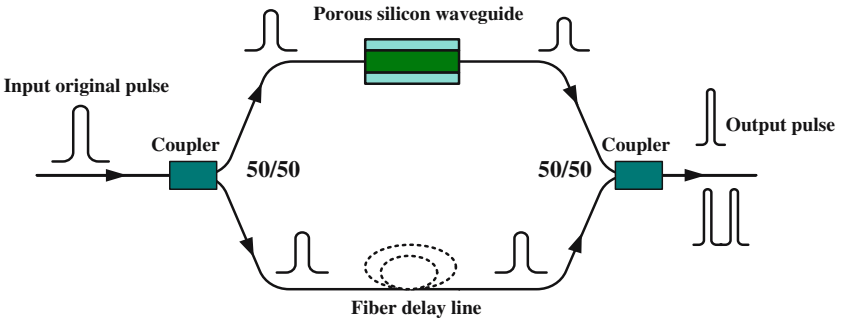

Figure 1. Schematic diagram of the proposed device for pulse generation and compression.

be achieved within proper delay time between the two output pulses. As a result, one can generate shorter single- or double-pulse by detuning the time delay, incident power, and pulse duration. Here, the coupled equations in the PS waveguide are given by [7]

$$\frac{\partial A(z,t)}{\partial z} = -\frac{1}{2}\alpha A(z,t) + i\gamma|A(z,t)|^2 A(z,t) - \frac{1}{2}\frac{\beta_T}{A_{eff}}|A(z,t)|^2 A(z,t) - \frac{1}{2}\sigma_{FCA}N(z,t)A(z,t) - i\frac{2\pi}{\lambda}k_{FCD}N(z,t)A(z,t) \quad (1)$$

$$\frac{dN(z,t)}{dt} = \frac{\beta_T}{2h\nu}\left(\frac{|A(z,t)|^2}{A_{eff}}\right)^2 - \frac{N(z,t)}{\tau_c}, \quad (2)$$

where A is the slowly varying envelope, z is the distance, α is the linear attenuation coefficient, γ is the Kerr nonlinear parameter, λ is the central wavelength of the input pulse, and A_{eff} is the effective area. β_T is the two-photon absorption coefficient, σ_{FCA} is the free carrier absorption cross-section, k_{FCD} is the free carrier dispersion coefficient, N is the free carrier density, and τ_c is the free carrier lifetime. The waveguide length $L = 3$ mm, the central wavelength of the initial pulse $\lambda = 1550$ nm, $n_2 = 2.3 \times 10^{-14}$ cm^2/W, $A_{eff} = 19.3\,\mu$m^2, $\beta_T = 0.8$ cm/GW, $\sigma_{FCA} = 100 \times 10^{-17}$ cm^2, $k_{FCD} = 90 \times 10^{-21}$ cm^3, $\alpha = 9$ dB/cm, $\tau_c = 0.2$ ns.

3. Results and discussion

A third-order super-Gaussian pulse as input beam is adopted in simulation, which has ∼40.3 W peak and 15.56 dB on-off ratio (10 log 10(logic 1/logic 0)), respectively. T_0, that is the time duration of half width at $1/e$ intensity point of the peak without considering pedestal energy is 1 ns. It is well known that, as the third-order super-Gaussian pulse is propagating along the PS waveguide, leading edge of the pulse experiences fast TPA process that results in a great deal of free carrier, and then the generated free carrier induced by TPA will absorb the photon of trailing edge of the pulse. As a result, the output pulse from the PS waveguide exhibits a long trailing edge [7]. Hence, the output pulse from the PS waveguide has very strong phase shift due to nonlinear effects of the waveguide. In addition, because, in the fibre delay line, the influences of linear and nonlinear effects on the pulse are ignored, the output pulse from the delay line does not have any change in phase and amplitude profiles. While two

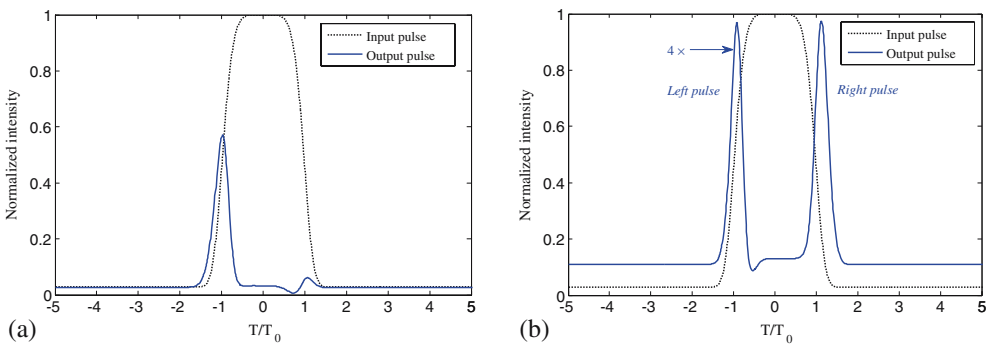

Figure 2. (**a**) Output single pulse with −235 ps delay and (**b**) output double-pulse with 235 ps delay.

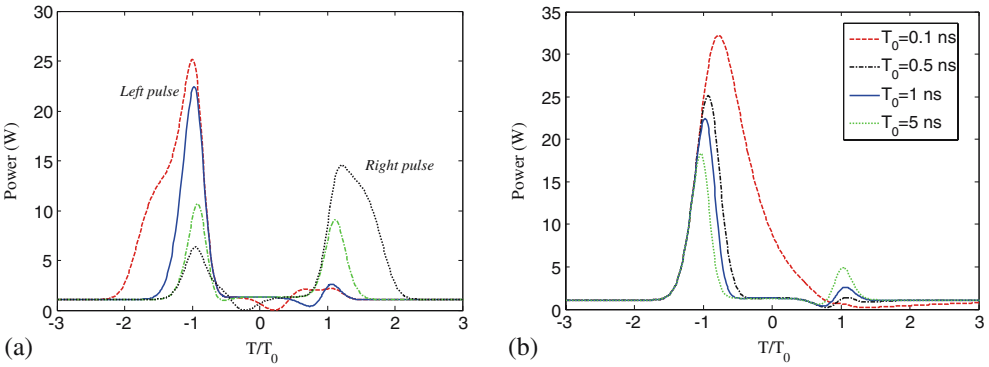

Figure 3. (**a**) Output pulse with various delay when $T_0 = 1$ ns and ∼40.3 W input peak and (**b**) output pulse with various initial pulse width when the delay is $-0.2T_0$ and the input peak is ∼40.3 W.

output pulses from delay line and PS waveguide are recombined at the output port of MZI, they have significant interference behaviour as a result of the strong phase difference so that one can achieve various output signals by judiciously detuning their delay time.

An output signal is indicated by the blue solid line in figure 2a, in which the delay time is −235 ps. Here, it should be pointed out that the negative delay time denotes that the output pulse from the fibre delay line reaches early the output coupler compared to the case of another output pulse from the PS waveguide. The full width at half maximum (FWHM) of the output pulse is compressed to ∼0.4 ns, which is about one-fifth of the time duration of the input pulse. This significant result is attributed to the interference effect between the two output pulses from the PS waveguide and fibre delay line. The maximum phase shift on top of the output pulse from the PS waveguide is around π that induces sufficient destructive interference with the result that the photon in the pulse trailing edge is strongly suppressed, and a compressed pulse shown in figure 2a is achieved. In contrast, if the delay time is tuned to 235 ps, a surprising phenomenon that displays double-pulse shape is observed in figure 2b, in which the positive delay time indicates that the output pulse from the delay line delays the output pulse from the PS waveguide when they reach the output port. Of course, the generated double-pulse is still a result of interference between two output pulses from MZI, whose time separation in the shape shown in figure 2b is about 2.043 ns, their time durations are as low as ∼0.34 ns (left pulse) and ∼0.40 ns (right pulse), respectively, and their peak heights are nearly equal. It is obvious that the delay time has important influence on the output pulse displayed in figure 3a, in which both single and double-pulse can be switched by tuning the delay time, −0.8 ns (red-dashed line), −0.2 ns (blue solid line), 0.2 ns (green dash–dot line), and 0.8 ns (black-dotted line). To discuss the influence of initial pulse width on the output signal, figure 3b shows the plots of the output pulse as the initial pulse width, T_0, varies from 0.1 ns to 5 ns. When $T_0 = 0.1$ ns, the output pulse takes on long tail owing to the free carrier

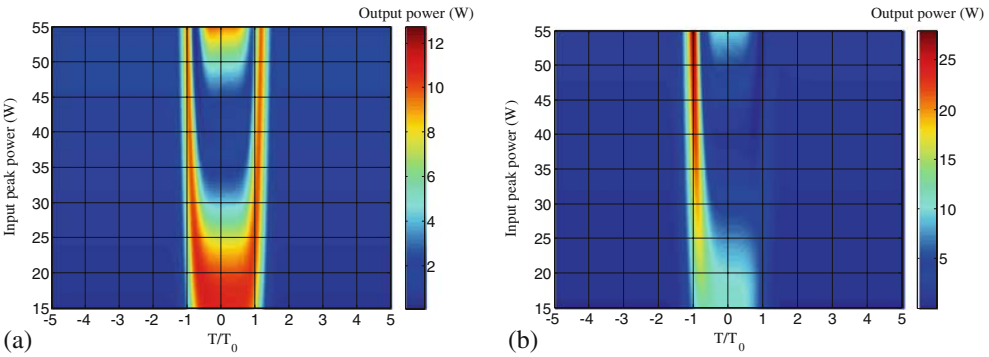

Figure 4. Pulse evolution against various input peak power for a delay of (**a**) 235 ps and (**b**) −235 ps.

absorption so that the output pulse exhibits strongly asymmetrical waveform, and its FWHM is shortened to ∼83.4 ps that is still less than T_0. However, while T_0 is extended to 0.5 ns, 1 ns, and 5 ns, some significant behaviours in the output pulses are observed owing to the broadened initial pulse width that is longer than the carrier lifetime, i.e., about five-fold compression pulse is generated compared to FWHM of the initial input pulse, and FWHM of the generated pulse is shortened to ∼0.23 ns, ∼0.48 ns, and ∼1.73 ns, respectively. With the increase in the initial pulse width, the pulse energy is increased under a fixed input peak power level, which will produce a great deal of excess carrier by two-photon absorption. Therefore, by the combined effects of two-photon absorption, free carrier related effects, and self-phase modulation, the propagation pulse will obtain enough phase shift in the PS waveguide so that both time duration and peak of the output pulse are significantly compressed due to the strong destructive interference and nonlinear absorption.

Obviously, the input peak power level directly results in nonlinear processes related to phase shift on the propagation beam in the PS waveguide. The output pulse evolution against various input peak is, respectively, displayed with delay of −235 ps and 235 ps in figures 4a and 4b, with ∼2 ns FWHM for the input pulse. If the input peak power is less than ∼25 W, the output pulse from the PS waveguide will not have enough phase shift. Therefore, the generated pulse is not effectively compressed, and double-pulse cannot be achieved. On the other hand, in the case of high input peak power (greater than ∼50 W), the corresponding maximum phase shift obviously overruns the value of π with the result that pedestal energy is remarkably enhanced due to interference effect. As a result, while the input peak power varies from ∼25 W to ∼50 W, high-quality single or double-pulse with short pulse width and suppressed pedestal energy is easily generated by selecting proper delay time.

4. Conclusions

A PS waveguide-based asymmetrical Mach–Zehnder interferometer has been presented in this work, in which a switching single- and double-pulse generation technique is presented and discussed. Time duration in the generated pulse is significantly compressed compared to that of the initial pulse. By introducing proper input peak power level and judiciously controlling the delay time between the two recombined pulses, one can easily switch the single-pulse or double-pulse output. It should be pointed out that, if the PS waveguide is replaced by other highly nonlinear waveguides, similar results can be obtained based on the configuration presented here.

Acknowledgements

The author acknowledges support from the National Natural Science Foundation of China (Grant No. 61205111). The authors would like to thank Prof. Amarendra K Sarma, Indian Institute of Technology Guwahati, for his suggestions to improve this paper and for useful discussions.

References

[1] H S Rong, A S Liu, R Jones, O Cohen, D Hak, R Nicolaescu, A Fang and M Paniccia, *Nature* **433**, 7023 (2005)
[2] M A Foster, A C Turner, J E Sharping, B S Schmidt, M Lipson and A L Gaeta, *Nature* **441**, 960 (2006)
[3] S M Gao, E K Tien, Q Song, Y W Huang and S K Kalyoncu, *Chin. Phys. Lett.* **27**, 124206 (2010)
[4] Y H Ding, B Huang, C Peucheret, J Xu, H Y Qu, X L Zhang and D X Huang, *Opt. Express* **22**, 6078 (2014)
[5] D C Zografopoulos, R Beccherelli and E E Kriezis, *Opt. Commun.* **285**, 3306 (2012)
[6] A Brimont, A M Gutierrez, M Aamer, D J Thomson, F Y Gardes, J M Fedeli, G T Reed, J Marti and P Sanchis, *IEEE Photon. J.* **4**, 1306 (2012)
[7] P Apiratikul, A M Rossi and T E Murphy, *Opt. Express* **17**, 3396 (2009)